Ral GTPases regulate neurite branching through GAP-43 and the exocyst complex

Giovanna Lalli and Alan Hall

Medical Research Council Laboratory for Molecular Cell Biology and Cell Biology Unit and Department of Biochemistry and Molecular Biology, University College London, London WC1E 6BT, England, UK

Neurite branching is essential for the establishment of appropriate neuronal connections during development and regeneration. We identify the small GTPase Ral as a mediator of neurite branching. Active Ral promotes neurite branching in cortical and sympathetic neurons, whereas Ral inhibition decreases laminin-induced branching. In addition, depletion of endogenous Ral by RNA interference decreases branching in cortical neurons. The two Ral isoforms, RalA and -B, promote branching through distinct pathways, involving the exocyst complex and phospholipase D, respectively. Finally, Ral-dependent branching is mediated by protein kinase C–dependent phosphorylation of 43-kD growth-associated protein, a crucial molecule involved in path-finding, plasticity, and regeneration. These findings highlight an important role for Ral in the regulation of neuronal morphology.

Introduction

Correct functioning of the nervous system depends on the establishment of precise connections between appropriate sets of neurons. A central challenge in neurobiology is therefore to define the mechanisms by which neurons innervate their targets. During early nervous system development, axons branch extensively as they navigate toward target cells and then again upon arrival at their destination. Dendrites also branch extensively, giving rise to characteristic dendritic trees able to influence the propagation of electric signals (Acebes and Ferrus, 2000; Luo, 2002).

The formation of neuronal branches depends on the ability of the cell cortex and cytoplasm of elongating neurites to undergo dynamic reorganization in response to extrinsic cues. The sprouting of new motile structures, such as filopodia and lamellae, is thought to be an early step in this process (Gallo and Letourneau, 2004). A variety of extracellular cues, such as neurotrophic factors, slits, ephrins, netrins, semaphorins, integrins, and cell adhesion molecules, can affect neurite branching (Acebes and Ferrus, 2000; Dent et al., 2004). The signals involved in establishing a branch point, however, are poorly understood. It is likely that neurite branching requires the coordination of multiple events, including actin polymerization, formation of new adhesive sites, changes to the microtubule cytoskeleton, and membrane delivery.

Correspondence to Alan Hall: alan.hall@ucl.ac.uk

Abbreviations used in this paper: cGAP-43, chick GAP-43; EGFP-F, farnesylated EGFP; GAP-43, 43-kD growth-associated protein; GEF, guanine nucleotide exchange factor; PLD, phospholipase D; RNAi, RNA interference; SCG, superior cervical ganglia; siRNA, small interfering RNA.

The online version of this article contains supplemental material.

The two Ral isoforms, RalA and -B, were originally associated with growth factor–induced Ras signaling pathways and are activated by a family of Ral guanine nucleotide exchange factors (GEFs), which includes Ral GDP dissociation stimulator, Rgl1, Rgl2, and Rlf (Quilliam et al., 2002). RalA and -B are found at the plasma membrane as well as on endocytic and exocytic vesicles, and they have been implicated in a variety of cellular processes, such as oncogenic transformation, transcriptional regulation, cell proliferation, vesicle trafficking, and cytoskeletal reorganization (Feig, 2003). Several effector molecules connect Ral with endocytic/exocytic pathways and cytoskeletal regulation. RalBP1, a Rac and Cdc42 GTPase-activating protein, also known as RLIP76, interacts with GTP-bound Ral and binds to proteins involved in clathrin-mediated endocytosis (Jullien-Flores et al., 2000). In addition, the association of Ral with phospholipase D (PLD) may play a role both in Golgi vesicle formation and in receptor-mediated endocytosis (Shen et al., 2001). Finally, the identification of the exocyst complex as a Ral effector has implicated this GTPase not only in the regulation of polarized membrane delivery (Moskalenko et al., 2002; Shipitsin and Feig, 2004) but also in Cdc42-dependent filopodia formation (Sugihara et al., 2002), suggesting that Ral has a role in the modulation of the actin cytoskeleton.

In neuronal cells, Ral has been found to be associated with cholinergic synaptic vesicles (Ngsee et al., 1991) and is involved in neurosecretion in PC12 cells (Moskalenko et al., 2002). Refilling of the readily releasable pool of synaptic vesicles is suppressed in transgenic mice expressing a dominant

The Journal of Cell Biology, Vol. 171, No. 5, December 5, 2005 857–869
http://www.jcb.org/cgi/doi/10.1083/jcb.200507061

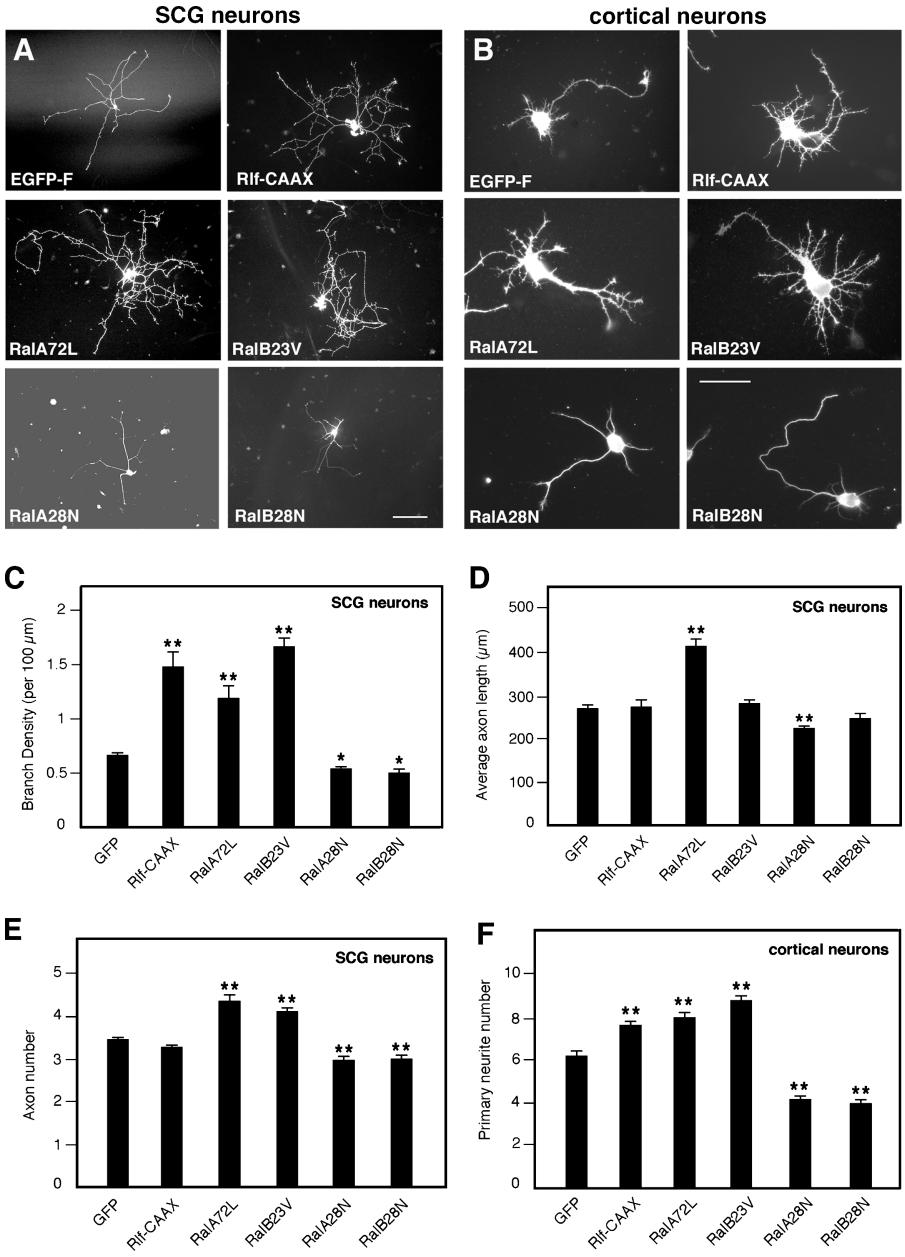

Figure 1. **Active Ral increases neurite branching.** SCG neurons (A) and cortical neurons (B) expressing EGFP-F or the indicated proteins visualized by anti-myc (for Ral) or anti-HA (for Rlf-CAAX) immunostaining. Pictures were taken 20 h after transfection. Constitutively active RalA (RalA72L) and -B (RalB23V) or the active Ral-GEF Rlf-CAAX increase neurite branching, whereas dominant-negative Ral (RalA28N and -B28N) decreases branching. SCG neurons were plated on laminin-coated dishes, whereas cortical neurons were grown on polyornithine. Bars: (A) 100 μm; (B) 50 μm. (C and D) Quantitative analysis of neurite morphology. Branch density per 100 μm of neurite length (C) is highly increased with Rlf-CAAX and constitutively active Ral and decreased with dominant-negative Ral (means ± SEM: GFP, 0.65 ± 0.03; Rlf-CAAX, 1.45 ± 0.14; RalA72L, 1.17 ± 0.12; RalB23V, 1.62 ± 0.09; RalA28N, 0.52 ± 0.03; RalB28N, 0.48 ± 0.03; **, $P < 0.0001$; *, $P < 0.01$). In contrast, average axon length (D) does not vary significantly, except for Ral A (means ± SEM: GFP, 261.62 ± 8.65; Rlf-CAAX, 266.41 ± 16.92; RalA72L, 402.54 ± 18.57; RalB23V, 274.53 ± 9.01; RalA28N, 216.89 ± 7.92; RalB28N, 238.74 ± 14.52; **, $P < 0.0001$). (E and F) Quantitative analysis of the number of primary neurites emerging from the cell body and containing microtubules in SCG neurons (means ± SEM: GFP, 3.38 ± 0.06; Rlf-CAAX, 3.20 ± 0.07; RalA72L, 4.25 ± 0.17; RalB23V, 4.03 ± 0.11; RalA28N, 2.91 ± 0.10; RalB28N, 2.93 ± 0.10; **, $P < 0.0001$) and cortical neurons (means ± SEM: GFP, 5.95 ± 0.23; Rlf-CAAX, 7.33 ± 0.18; RalA72L, 7.67 ± 0.26; RalB23V, 8.42 ± 0.25; RalA28N, 3.98 ± 0.20; RalB28N, 3.78 ± 0.18; **, $P < 0.0001$).

inhibitory form of RalA (Polzin et al., 2002). In addition, Ral associates with PLD2 and class 1 metabotropic glutamate receptors 1a and 5a in the adult rat brain and may regulate their constitutive endocytosis (Bhattacharya et al., 2004). Finally, Ral activation has been shown to delay NGF-induced neurite outgrowth in PC12 cells (Goi et al., 1999), but the connection between Ral and cytoskeletal remodeling in neurons has yet to be determined.

We report that Ral regulates neurite branching in cortical and sympathetic neurons. Activation of Ral leads to increased branching, whereas inhibition blocks integrin-mediated neurite branching. RalA and -B promote branching through two different pathways involving the exocyst complex and PLD, and the latter leads to PKC-dependent phosphorylation of 43-kD growth-associated protein (GAP-43), which is implicated in branching and axonal regeneration (Oestreicher et al., 1997; Bomze et al., 2001).

Results

Active Ral increases neurite branching

To determine whether Ral GTPases are able to influence neuronal morphology, we microinjected sympathetic superior cervical ganglia (SCG) neurons (Fig. 1 A) or nucleofected cortical neurons (Fig. 1 B) with constitutively active Ral (RalA72L and -B23V), dominant-negative Ral (RalA28N and -B28N), or Rlf-CAAX, a constitutively active Ral-GEF (Wolthuis et al., 1997). SCG neurons were microinjected 2 h after plating, when only short neurites growing from somata were visible, whereas cortical neurons were nucleofected before plating. A farnesylated version of EGFP (EGFP-F) was used to visualize neuronal morphology. Protein expression was confirmed by staining cells with anti-myc or anti-HA antibodies for Ral and Rlf, respectively (Fig. 1, A and B). SCG neurons tend to extend only long

processes, whereas cortical neurons adopt a typical polarized morphology with several short neurites and a single longer, axonlike process. Expression of constitutively active Ral isoforms or activation of endogenous Ral with Rlf-CAAX in both types of neuron enhanced cell body spreading and branching complexity (Fig. 1, A and B, top right and middle). Quantification revealed a dramatic increase of branch density, ranging from 80 to 150%, in cells expressing constitutively active Ral or Rlf-CAAX compared with control cells expressing EGFP (Fig. 1 C), whereas cells expressing dominant-negative Ral were characterized by a decreased number of branches and a significant (20–25%) decrease in branch density (Fig. 1, A and B [bottom] and C). Rlf-ΔCAT-CAAX, a Rlf-CAAX control construct lacking catalytic activity (Wolthuis et al., 1997), did not affect branching (unpublished data). The average axon length did not change significantly when expressing Rlf-CAAX (Fig. 1 D), indicating that activation of endogenous Ral proteins induces a specific effect on branching. Interestingly, constitutively activated and dominant-negative RalA, but not -B, also had an effect on axon length in SCG neurons (Fig. 1 D), whereas both isoforms had an effect on the number of primary neurites per cell in both SCG and cortical neurons (Fig. 1, E and F). These results suggest that Ral may play other roles in addition to branching.

Depletion of endogenous Ral by RNA interference (RNAi) decreases branching

To gain further evidence for a role of Ral in neurite branching, we depleted cortical neurons of RalA, RalB, or both by RNAi. Small interfering RNA (siRNA) duplexes against RalA, RalB, or both were introduced in freshly dissociated cortical neurons by nucleofection. Cells were plated, fixed, and stained 50 h later for the Ral isoforms and for tubulin to visualize microtubules. Control cells nucleofected with a scramble siRNA duplex directed against GFP showed a typical polarized morphology, with short neurites and a major process extending from the cell body. All these neurites display a certain branching complexity, as visualized by the microtubule staining (Fig. 2 A, right). In these cells, endogenous RalA is abundant and equally distributed in all neurites (Fig. 2 A, left), whereas RalB appears to be especially concentrated in the terminal portion of major neurites (Fig. 2 A, middle). Neurons transfected with the siRNA against RalA displayed a general decrease in RalA immunoreactivity, whereas RalB staining remained (Fig. 2 B, left and middle). The opposite effect was observed with the siRNA against RalB (Fig. 2 C, left and middle). Importantly, in both cases, neurons were characterized by a simpler branching morphology compared with controls (Fig. 2, compare the tubulin stainings in B and C [right] with those in A [right]). Finally, RNAi of both Ral isoforms also led to a substantial decrease in neurite branching (Fig. 2 D).

Western blot analysis revealed a 60–70% decrease in RalA levels after siRNA treatment (Fig. S1 A, available at http://www.jcb.org/cgi/content/full/jcb.200507061/DC1). However, we were unable to quantify the reduction in RalB after siRNA treatment because the RalB antibody cross reacts with RalA on Western blots (Fig. S1 B; unpublished data), though not in immunofluorescence (Fig. 2, A–D). Transfection of both RalA and -B siRNA led to an ~90% decrease of total Ral levels (Fig. S1 B).

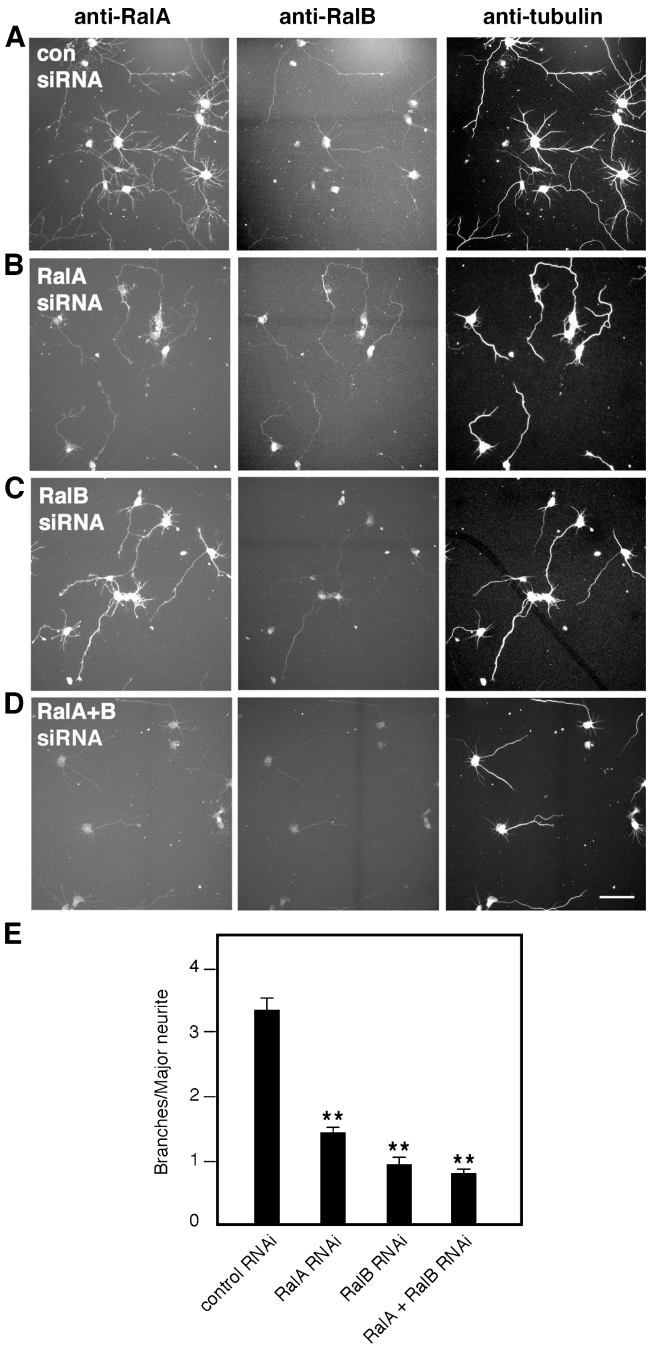

Figure 2. **Depletion of endogenous Ral by RNAi decreases branching.** Cortical neurons fixed and stained for RalA, RalB, and tubulin 50 h after nucleofection of the indicated siRNA duplexes. (A) Neurons nucleofected with control siRNA display branched neurites visualized by the tubulin staining. RNAi of RalA (B), RalB (C), and both Ral isoforms (D) decreases branching complexity, particularly in major neurites. Bar, 50 μm. (E) Quantitative analysis of branching from major neurites of cortical neurons after RNAi for RalA, RalB, or both Ral isoforms (means ± SEM: control RNAi, 3.39 ± 0.19; RalA RNAi, 1.41 ± 0.11; RalB RNAi, 0.91 ± 0.13; RalA + RalB RNAi, 0.77 ± 0.09; **, $P < 0.0001$).

We quantified the number of branches containing microtubules and extending from the major neurite of isolated cortical neurons. RalA and -B RNAi caused a 57 and 70% decrease in branching, respectively, whereas simultaneous RNAi for both Ral isoforms led to a 75% decrease in branch number (Fig. 2 E).

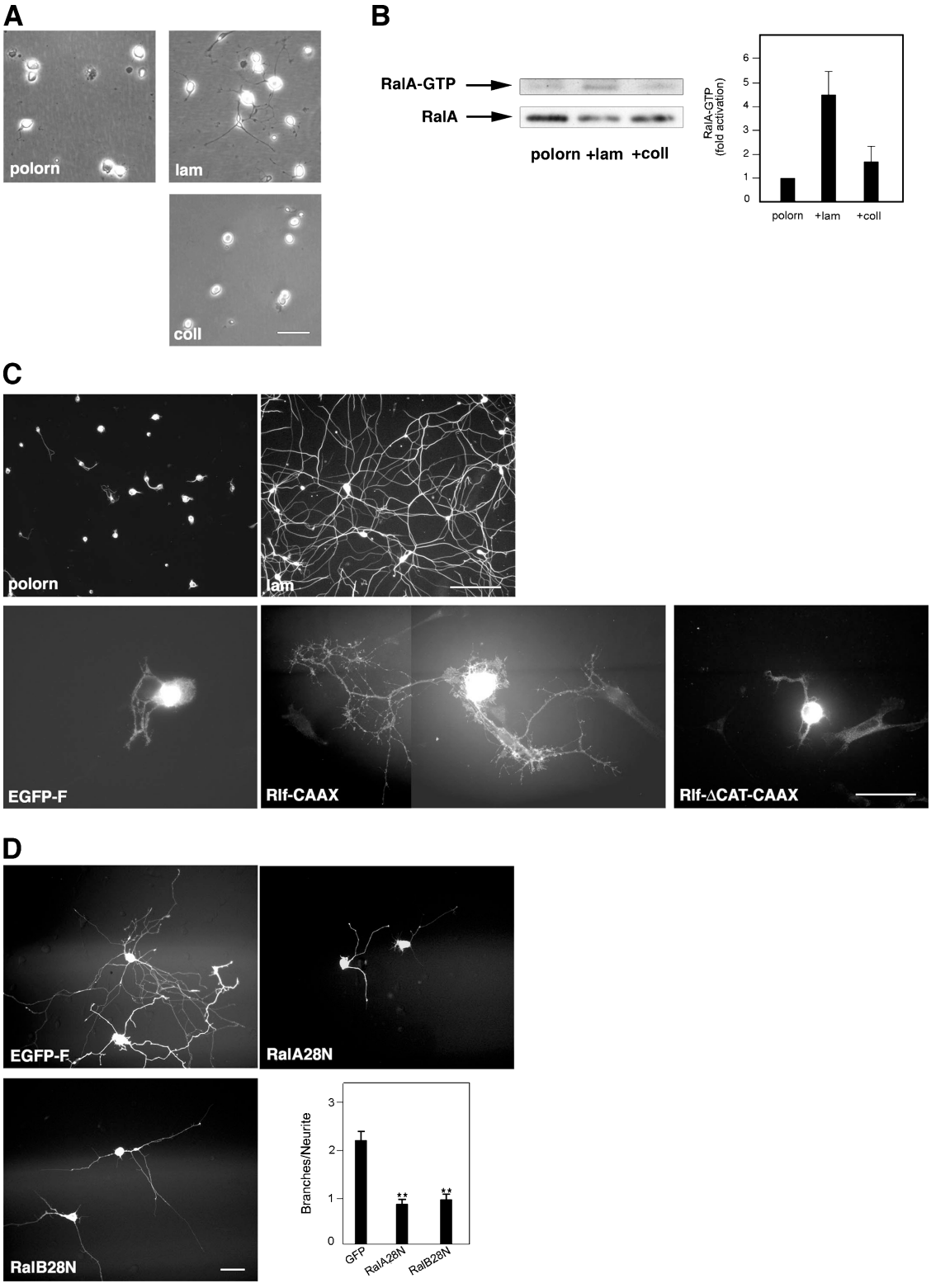

Figure 3. **Ral is activated by laminin and is required for neurite branching promoted by laminin.** (A) Phase-contrast pictures of SCG neurons taken 3 h after plating on polyornithine (polorn), polyornithine and laminin (lam), or polyornithine and collagen (coll). Note the visible neurite outgrowth and branching of the laminin-plated neurons compared with cells growing on the other substrates. Bar, 20 μm. (B) SCG neurons were lysed 3 h after plating on the indicated substrates. The amount of RalA-GTP in the lysates was determined by affinity purification with the Ral binding domain of RalBP1 and immunoblotting with anti-RalA antibodies. A representative blot is shown (left), together with the quantification of data of three independent experiments (right; means ± SEM; *, $P < 0.005$). (C, top) SCG neurons stained for tubulin and photographed 24 h after plating on polyornithine or polyornithine and laminin. Cells plated on polyornithine show limited neurite outgrowth and branching compared with neurons growing on laminin. Bar, 100 μm. (bottom) SCG neurons plated on polyornithine and expressing Rlf-CAAX display extensive branching (middle), an effect absent in neurons expressing EGFP-F (left) or inactive Rlf (Rlf-ΔCAT-CAAX; right). Bar, 50 μm. (D) SCG neurons plated on polyornithine were left to express the indicated proteins for 5 h before laminin addition. Pictures were taken after overnight expression. Neurite branching triggered by laminin as observed in cells expressing EGFP-F (top left) is impaired in neurons expressing

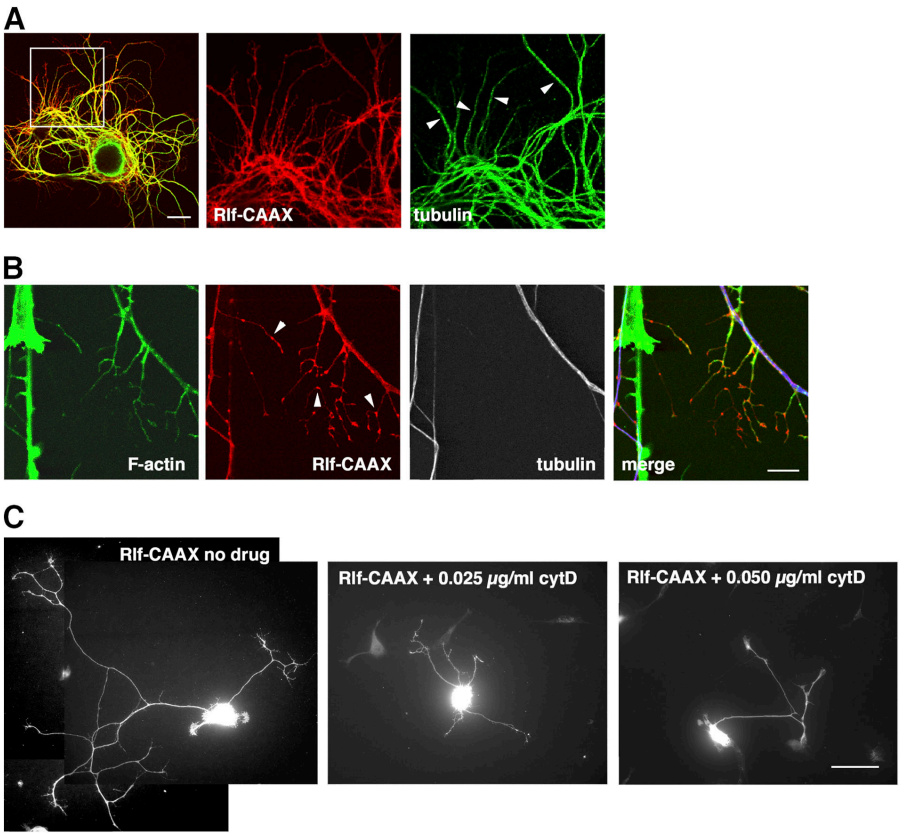

Figure 4. **Branches induced by Ral activation depend on F-actin.** (A, left) Confocal image of an SCG neuron plated on polyornithine expressing Rlf-CAAX (red) and stained for tubulin (green). The middle and right panels are enlargements of the boxed area in the left panel. Longer branches are positive for tubulin (arrowheads). Bar, 20 μm. (B) In Rlf-CAAX–expressing neurons, short branches contain actin filaments visualized by fluorescent phalloidin (green) but not tubulin (white, blue in the merge panel). Note the accumulation of Rlf-CAAX (red) in discrete domains along branches (arrowheads). Bar, 10 μm. (C) Representative images of SCG neurons plated on polyornithine, expressing Rlf-CAAX, and treated with the indicated amounts of cytochalasin D. Increasing drug doses led to a progressive block of Ral-dependent branching. Bar, 50 μm.

Together, these results strongly support a role for both Ral isoforms in promoting neurite branching.

Ral is required for laminin-induced neurite branching

Because integrin activation has been implicated in the regulation of neurite outgrowth and branching (Ivins et al., 2000), we tested the influence of different substrates on the levels of Ral activation. SCG neurons were plated on plastic dishes coated with polyornithine only or polyornithine plus either laminin or collagen. 3 h after plating, neuronal morphology varied according to the substrate (Fig. 3 A). SCGs plated on collagen or on polyornithine appeared mainly round with very short processes (Fig. 3 A, top left and bottom). In contrast, cells growing on laminin had longer, branched neurites (Fig. 3 A, top right). To quantify the levels of active Ral under these different conditions, we used a fragment of RalBP1 known to preferentially bind to Ral-GTP as an affinity reagent (Tian et al., 2002). Ral-GTP levels in neurons plated on laminin were approximately fourfold higher than on the other substrates, whereas the total amount of Ral in lysates from different samples was comparable (Fig. 3 B).

24 h after plating on polyornithine, SCG neurons extend only short neurites, whereas in the presence of laminin, they form a highly branched network (Fig. 3 C, compare top left and right panels). We tested whether activation of endogenous Ral could bypass the requirement for laminin. Rlf-CAAX induced a dramatic branched morphology in the majority of injected cells plated on polyornithine (Fig. 3 C, bottom middle), though neurite length was shorter compared with cells plated on laminin. Importantly, cells expressing EGFP-F or Rlf-ΔCAT-CAAX showed only short neurites (Fig. 3 C, bottom left and right). To determine whether Ral activity is necessary for laminin-induced neurite branching, we microinjected SCG neurons plated on polyornithine with dominant-negative Ral, waited for at least 4 h to allow protein expression, and triggered neurite extension overnight by adding laminin to the medium. Neurite extension still occurred, but branching was dramatically impaired compared with neurons expressing EGFP-F (Fig. 3 D). We conclude that active Ral is required for laminin-induced neurite branching.

Cytoskeletal characterization of Ral-induced neurite branches

Neurite branching requires reorganization of the cytoskeleton and is generally initiated by the appearance of motile filopodia in response to extracellular cues (Gallo and Letourneau, 2004). We stained the Ral-induced branches with fluorescent phalloidin to visualize actin filaments and an anti-tubulin antibody to reveal microtubules. In SCG neurons expressing Rlf-CAAX, phalloidin labeled filopodia, short nascent branches, and long branches, but microtubules could be detected only in longer branches (Fig. 4, A and B). Notably, Rlf-CAAX appeared to be concentrated in puncta along neurites and sprouting branches and was often

dominant-negative Ral isoforms (top right and bottom left). (bottom right) A quantitative analysis of neurite branching in five independent laminin-addition experiments (means ± SEM: GFP, 2.19 ± 0.18; RalA28N, 0.84 ± 0.09; RalB28N, 0.95 ± 0.10; **, $P < 0.0001$). Bar, 30 μm.

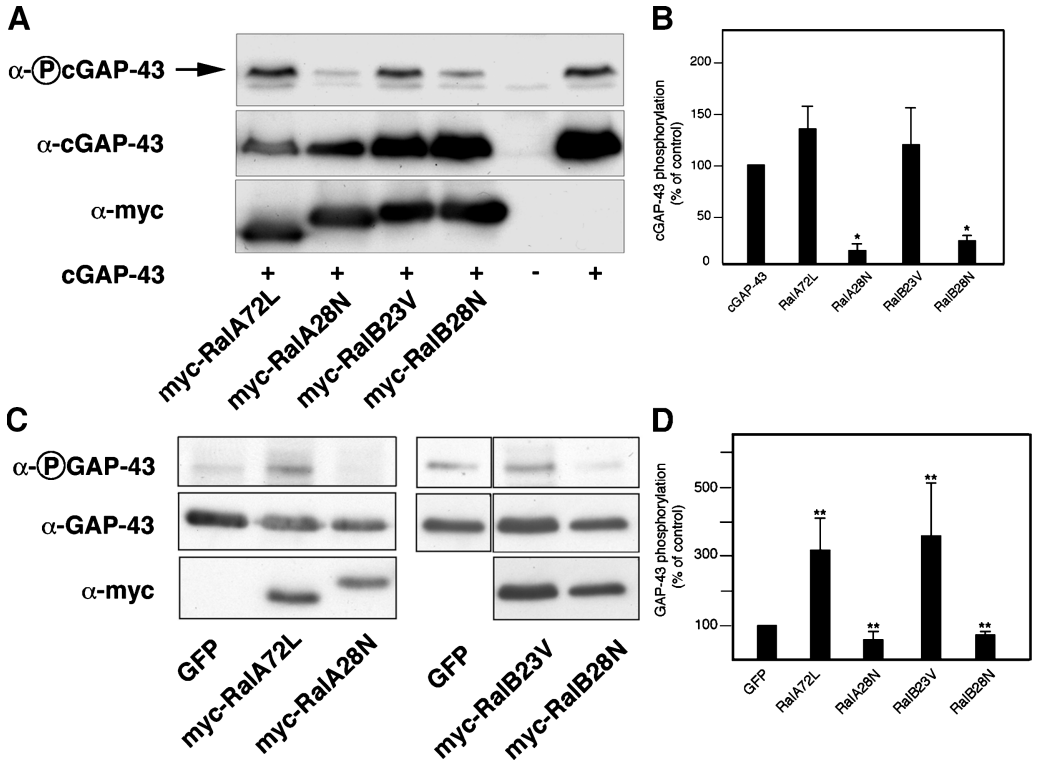

Figure 5. **Ral regulates GAP-43 phosphorylation.** (A) COS cells were transfected with the indicated myc-tagged Ral constructs and cGAP-43. Levels of phospho-cGAP-43 in cell extracts were determined by immunoblotting with an anti–phospho-GAP-43 antibody. A representative blot is shown. Inactive Ral causes a significant decrease of cGAP-43 phosphorylation (top band, arrow). (B) Quantitative analysis of phosphorylated cGAP-43 in COS cells transfected with cGAP-43 and the indicated Ral constructs. Shown here are data from four independent experiments (means ± SEM; *, $P < 0.01$). (C) Cortical neurons were nucleofected with the indicated constructs and lysed after overnight expression. Levels of total and phosphoendogenous GAP-43 were then assessed by immunoblotting. The fourth, fifth, and sixth lanes were derived from the same blot. (D) Quantitative analysis of endogenous GAP-43 phosphorylation in cortical neurons after nucleofection with the indicated Ral mutant isoforms. Data were derived from four independent experiments (means ± SEM; **, $P < 0.005$).

present at branch points (Fig. 4 B, arrowheads). SCG neurons expressing constitutively active Ral showed clear filopodial sprouting also from cell bodies (Fig. S2, available at http://www.jcb.org/cgi/content/full/jcb.200507061/DC1). Treatment of neurons with cytochalasin D, an inhibitor of actin polymerization, blocked filopodial sprouting and branching in a dose-dependent manner (Fig. 4 C). These observations suggest that active Ral causes branching by promoting the formation of filopodia and then allowing microtubules to invade the branch, consistent with previous studies on branch initiation (Dent et al., 2003; Gallo and Letourneau, 2004).

Ral modulates phosphorylation of GAP-43

In our search for molecules that could act downstream of Ral to promote branching, we focused on GAP-43, a neuronal protein known to promote the formation and growth of local branches in target regions of innervation (Aigner et al., 1995) but also able to induce filopodia in various cell types (Widmer and Caroni, 1993). Phosphorylation of GAP-43 on Ser41 by PKC and its membrane anchoring through palmitoylation of cysteine residues at the NH_2 terminus promote cytoskeletal remodeling (Widmer and Caroni, 1993; Aigner et al., 1995). Because PKC-dependent phosphorylation at Ser41 is associated with sprout-promoting activity (Aigner et al., 1995) and adhesion to laminin stimulates GAP-43 phosphorylation (Fig. S3, available at http://www.jcb.org/cgi/content/full/jcb.200507061/DC1), we determined whether Ral could affect the phosphorylation state of this residue in GAP-43. COS cells were first cotransfected with Ral mutants and an epitope-tagged chick version of GAP-43 (cGAP-43; Widmer and Caroni, 1993). In chick, the PKC phosphorylation site of GAP-43 is Ser42, corresponding to Ser41 in mammalian GAP-43 (Widmer and Caroni, 1993). Levels of phosphorylated cGAP-43 were then monitored by immunoblotting (Fig. 5 A). Dominant-negative Ral substantially decreased GAP-43 phosphorylation. In contrast, active Ral had little effect (Fig. 5 B), possibly because of intrinsically high levels of PKC activity in COS cells. To test the ability of Ral to modulate GAP-43 phosphorylation in primary neurons, we measured levels of endogenous phosphorylated GAP-43 in cortical neurons 24 h after nucleofection with Ral mutants. Efficiency of nucleofection in these cells was between 50 and 70%, and myc-tagged Ral was detected by immunoblotting (Fig. 5 C). Quantitative analysis showed that dominant-negative Ral significantly decreased phosphorylation of endogenous GAP-43, whereas active Ral caused a threefold increase (Fig. 5 D). In addition, phosphorylation of endogenous GAP-43 significantly decreased in neurons depleted of Ral by nucleofection of RalA and -B siRNA (Fig. S4 A). Finally, treatment with

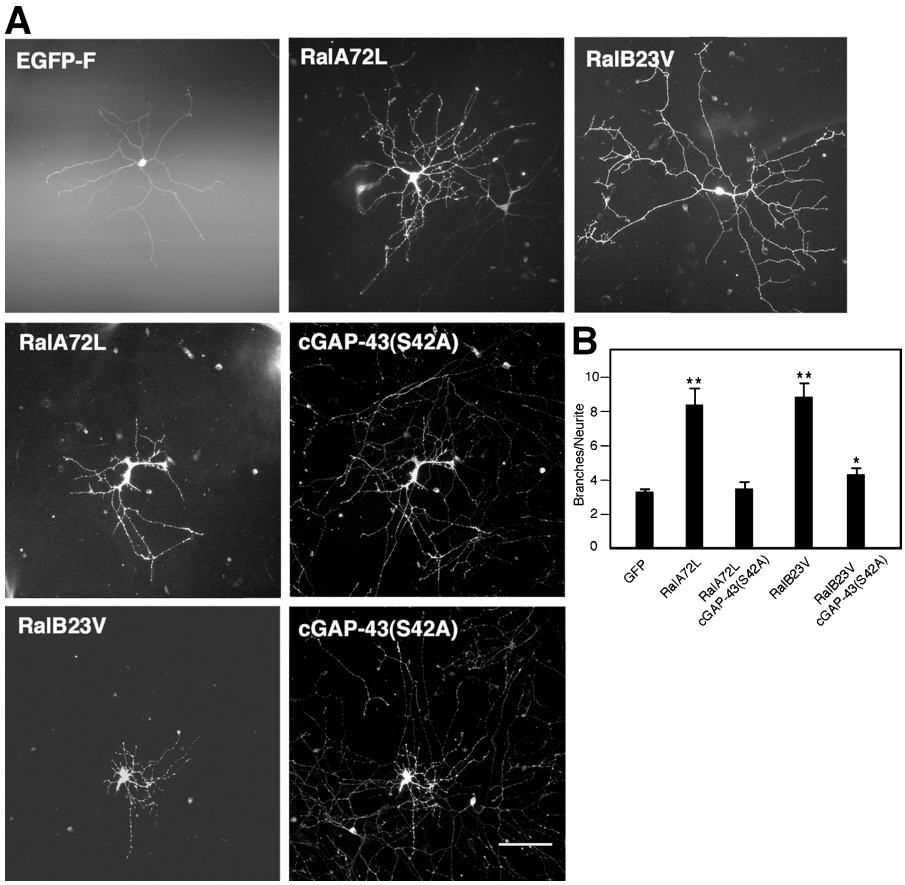

Figure 6. **GAP-43 acts downstream of Ral.** (A) Constitutively active Ral increases branching in neurons plated on laminin (top middle and right) compared with EGFP-F–expressing cells (top left). This effect is reduced by coexpression of cGAP-43(S42A) (middle and bottom). Shown here are cells stained with anti-myc antibody to detect mutant Ral and anti–cGAP-43. Bar, 100 μm. (B) Quantitative analysis of branching in cells injected with single Ral isoforms or with Ral and cGAP-43(S42A) (means ± SEM: GFP, 3.30 ± 0.18; RalA72L, 8.43 ± 0.97; RalA72L + cGAP-43(S42A), 3.55 ± 0.44; RalB23V, 8.88 ± 0.85; RalB23V + cGAP-43(S42A), 4.29 ± 0.41; *, $P < 0.02$; **, $P < 0.0001$).

the PKC inhibitor GF109203X completely blocked the enhanced phosphorylation of endogenous GAP-43 caused by active Ral (Fig. S4 B). We conclude that Ral regulates PKC-mediated phosphorylation of GAP-43 on Ser41.

To further test this conclusion, constitutively active Ral and a cGAP-43 mutant that cannot be phosphorylated on Ser42 (S42A; Widmer and Caroni, 1993) were coinjected in SCG neurons plated on laminin. The striking increase in branching caused by active Ral was blocked (Fig. 6, A and B). Finally, a phosphomimetic mutant of cGAP-43 (S42D; Widmer and Caroni, 1993) was able to fully rescue the decreased branching caused by inhibition of RalB in cells plated on laminin (Fig. 7, A and B). Interestingly, rescue of inhibition of the RalA isoform was only partial (Fig. 7, A and B). In contrast, wild-type cGAP-43 did not rescue the effects of dominant-negative Ral (unpublished data). Similar results were obtained for neurons initially plated on polyornithine, microinjected, and left to express for a few hours before laminin addition (Fig. 7, C and D). Together, these results place GAP-43 downstream of an integrin- and Ral-dependent pathway leading to neurite branching.

RalA and -B regulate branching through different effectors

Along with published data from others, the results in Fig. 7 raise the possibility that RalA and -B preferentially activate different downstream pathways (Chien and White, 2003; Shipitsin and Feig, 2004). To determine whether multiple effectors are responsible for Ral-induced neurite branching, we used Ral mutants previously identified on the basis of their loss of binding affinity for specific effector proteins. In particular, we used myc-tagged constitutively active RalA and -B isoforms unable to bind the Sec5 and Exo84 exocyst complex subunits (RalA72LD49E and -B23VD49E; Moskalenko et al., 2002, 2003) or selectively uncoupled from RalBP1 (RalA72LD49N and -B23VD49N; Jullien-Flores et al., 2000). We also used active Ral mutants lacking the NH_2-terminal 11 amino acids (RalA72LΔN11 and -B23VΔN11), which are required for association with PLD (Jiang et al., 1995). SCG neurons plated on laminin were microinjected either with EGFP-F as control or with active RalA, RalB, or the Ral effector domain mutants. Cells were fixed 24 h after injection and stained with anti-myc antibodies. As expected, active RalA and -B increased branching compared with EGFP-F (Fig. 8, A–C, compare EGFP-F, RalA72L, and RalB23V). The RalA mutant unable to interact with PLD showed a small but significant reduction in branch-promoting ability, whereas the mutant uncoupled from RalBP1 was as effective as active RalA (Fig. 8, B and C, compare RalA72L with RalA72LΔN11 and RalA72LD49N). Remarkably, however, preventing the interaction of active RalA with the exocyst complex dramatically inhibited its ability to promote branching (Fig. 8, B and C, compare RalA72L with RalA72LD49E). Interestingly, the RalB mutants unable to interact with either the exocyst complex or RalBP1 promoted branching similarly (if not better) to active RalB (Fig. 8, B and C, compare RalB23V with RalB23VD49E and RalB23VD49N). In contrast, the RalB mutant unable to interact with PLD displayed a significant de-

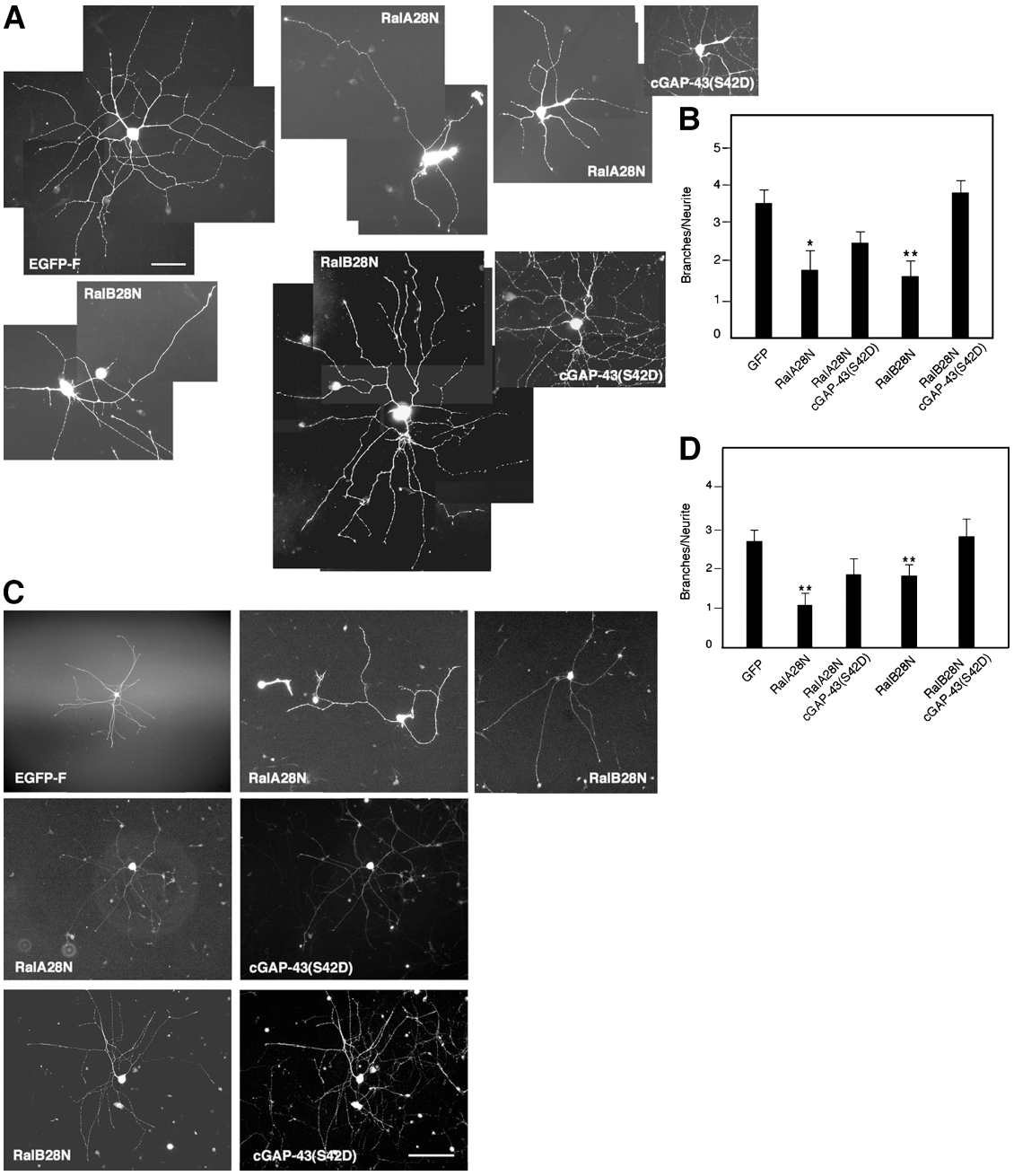

Figure 7. **GAP-43 acts downstream of Ral.** (A) A phosphomimetic GAP-43 protein, cGAP-43(S42D), restores branching in neurons plated on laminin and expressing dominant-negative Ral. Shown here are neurons expressing EGFP-F (top left), RalA28N (top middle), or RalB28N (bottom left) and RalA28N or RalB28N and cGAP-43(S42D) (right). Cells are stained with an anti-myc antibody to detect mutant Ral and an anti–cGAP-43 antibody. Bar, 50 μm. (B) Quantitative analysis of branching in cells plated on laminin and injected with single Ral isoforms or with Ral and cGAP-43(S42D) (means ± SEM: GFP, 3.47 ± 0.37; RalA28N, 1.74 ± 0.52; RalA28N + cGAP-43(S42D), 2.42 ± 0.31; RalB28N, 1.56 ± 0.41; RalB28N + cGAP-43(S42D), 3.72 ± 0.35; *, $P < 0.04$; **, $P < 0.001$). (C) SCG neurons were plated on polyornithine, microinjected, and left to express the indicated proteins for 5 h before laminin addition. Expression of dominant-negative Ral decreases branching compared with EGFP-F–expressing cells (top, compare middle and right with left). Branching is restored in cells coexpressing cGAP-43(S42D) (middle and bottom rows). Bar, 100 μm. (D) Quantitative analysis of branching in neurons initially plated on polyornithine and injected with single Ral isoforms or with Ral and cGAP-43(S42A) before laminin addition (means ± SEM: GFP, 2.64 ± 0.35; RalA28N, 1.05 ± 0.32; RalA28N + cGAP-43(S42D), 1.82 ± 0.40; RalB28N, 1.74 ± 0.30; RalB28N + cGAP-43(S42D), 2.73 ± 0.45; **, $P < 0.01$).

crease in branch-promoting activity (Fig. 8, A–C, compare RalB23VΔN11 with RalB23V and EGFP). To provide additional support for a role for PLD in Ral-induced branching, SCG neurons were incubated with 0.4% 1-butanol, a PLD inhibitor (Morris et al., 1997), after injection with active Ral. This treatment significantly abolished RalA- and completely blocked RalB-dependent increases in branching, whereas incubation with 0.4% 2-butanol, as a control, had no effect (Fig. 8 D). Together, these results indicate that Ral may increase neurite branching through the exocyst complex and PLD.

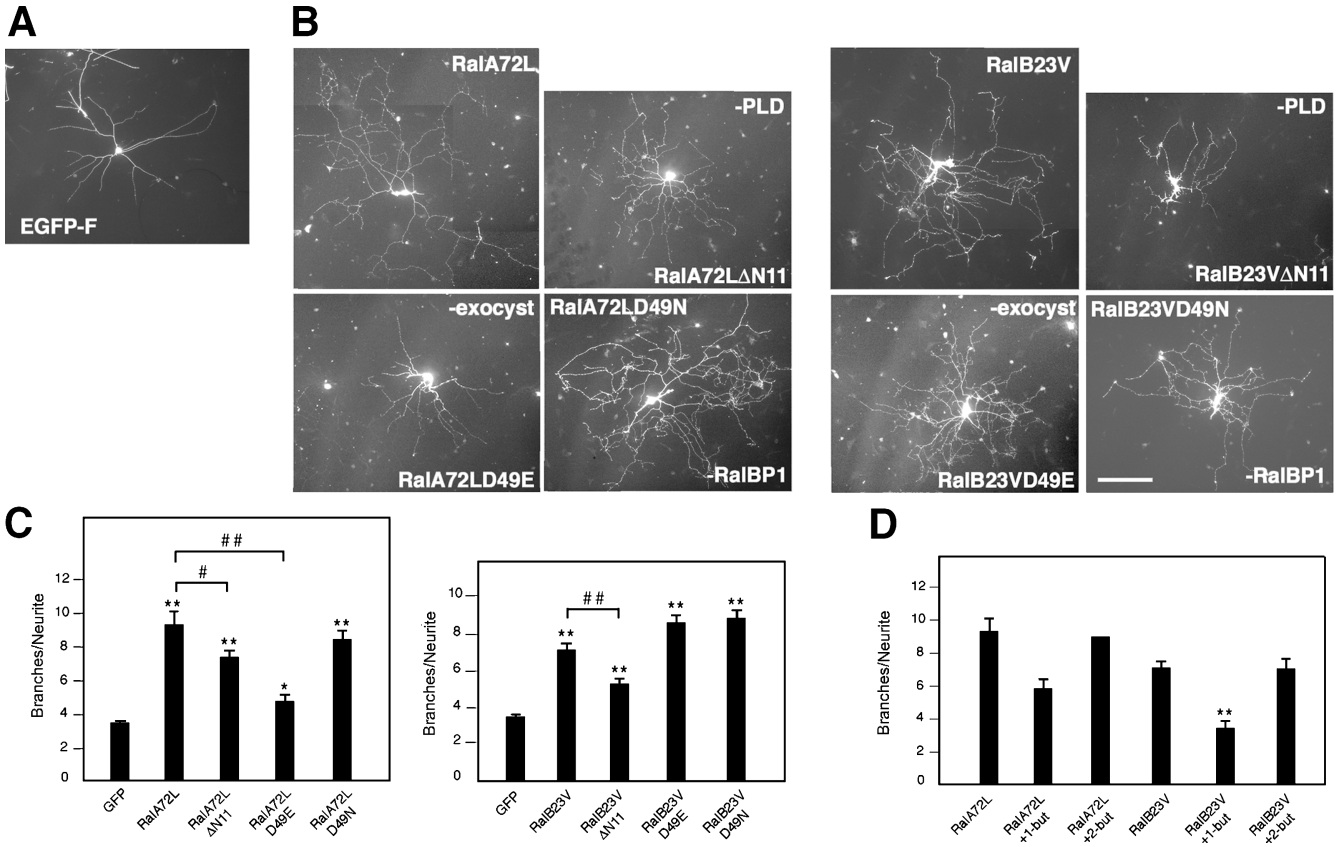

Figure 8. **Branching is mediated by distinct RalA and -B effectors.** (A) An SCG neuron expressing EGFP-F 24 h after microinjection. (B) SCG neurons expressing the indicated proteins visualized by anti-myc immunostaining. Active RalA (RalA72L) increases branching, but this effect is particularly impaired in cells expressing active RalA unable to interact with the exocyst complex (RalA72LD49E). The increased branching caused by active RalB (RalB23V) is inhibited in neurons expressing active RalB unable to associate with PLD (RalB23VΔN11). Other RalB effector domain mutants retain branch-promoting activity. Bar, 100 μm. (C) Quantitative analysis of branching for control cells expressing EGFP-F, active RalA or -B, and their effector mutants (means ± SEM: GFP, 3.44 ± 0.13; RalA72L, 9.34 ± 0.83; RalA72LΔN11, 7.37 ± 0.45; RalA72LD49E, 4.68 ± 0.43; RalA72LD49N, 8.43 ± 0.59; RalB23V, 7.09 ± 0.42; RalB23VΔN11, 5.26 ± 0.34; RalB23VD49E, 8.62 ± 0.48; RalB23VD49N, 8.83 ± 0.47; *, $P < 0.006$; **, $P < 0.0001$; #, $P < 0.03$; ##, $P < 0.0001$). (D) Quantitative analysis of branching in cells expressing active RalA or -B and incubated with 0.4% 1-butanol or 2-butanol. PLD inhibition by 1-butanol abolishes the effect of RalB on branching while partially inhibiting the increased branching caused by RalA. Control treatment with 2-butanol does not affect the branch-promoting activity of either Ral isoform (means ± SEM: RalA72L, 9.34 ± 0.83; RalA72L + 1-but, 5.78 ± 0.62; RalA72L + 2-but, 9.12 ± 0.08; RalB23V, 7.09 ± 0.42; RalB23 + 1-but, 3.34 ± 0.47; RalB23V + 2-but, 7.04 ± 0.66; **, $P < 0.0001$).

Discussion

We report in this paper that activation of Ral by integrin signaling increases neurite branching through pathways involving the exocyst complex, PLD activation, and PKC-mediated phosphorylation of GAP-43. To date, there have been only few studies on the function of Ral in neurons. Inhibition of Ral has been reported to enhance NGF-mediated neurite outgrowth in PC12 cells and, although this seems contradictory to the results reported here, it is likely that this may have had more to do with inhibition of the differentiation program than with cytoskeletal changes (Goi et al., 1999). A previous study in synaptosomes isolated from transgenic mice expressing dominant-negative RalA implicated Ral in the regulation of neurosecretion (Polzin et al., 2002). Interestingly, these authors showed that dominant-negative Ral suppressed both phorbol ester– and calcium-induced phosphorylation of known PKC substrates, such as MARCKS and SNAP-25. The animals did not display any gross morphological defects in the brain, but the use of the neuronal-specific enolase promoter, which becomes active in mature neurons only at the time of synaptogenesis, may have prevented the discovery of potential defects in neuronal morphology during development. Cortical neurons expressing dominant-negative Ral maintain a polarized morphology with an axonlike process and a few shorter neurites, suggesting that Ral activity is dispensable for the establishment of neuronal polarity. Indeed, we still observe neurite growth in both cortical and SCG neurons expressing dominant-negative Ral, indicating that this GTPase is not necessary for neurite extension per se. Ral activation may instead be associated with local signaling events required during development and leading to branching, such as axon pathfinding, formation of terminal arborizations, and lesion-induced neurite sprouting.

We show that both RalA and -B promote phosphorylation of GAP-43 but only RalA acts through the exocyst complex. These results indicate that the two Ral isoforms may promote branching by different mechanisms; in support of this, expression of Rlf-CAAX, a Ral-GEF able to activate both endogenous RalA and -B, produced the most striking effect on branching. In addition, knocking down a single Ral isoform by RNAi pro-

duced a significant decrease in branching, indicating that RalA and -B may play distinct roles in regulating branch number. RalA has been reported to bind to the exocyst complex more effectively than active RalB both in vitro and in cultured cells (Shipitsin and Feig, 2004). Even though the two Ral isoforms are 85% identical, they differ in their COOH-terminal domain, which is responsible for their distinct cellular localization, as shown in MDCK cells (Shipitsin and Feig, 2004). It is possible that the different localization of Ral isoforms could differentially modulate their interaction with various effectors.

Disrupting the interaction of RalA with the exocyst impaired the ability of active RalA to promote branching, implying that the exocyst plays an important role in branching. Previous papers have implicated the exocyst, a complex consisting of at least eight subunits, in cytoskeletal regulation. Interaction between RalA and the exocyst complex has been shown to mediate Cdc42-dependent filopodia formation in fibroblasts (Sugihara et al., 2002). PC12 cells expressing dominant-negative sec10 and ventral cord neurons from *sec5* mutant *Drosophila melanogaster* larvae fail to extend neurites (Vega and Hsu, 2001; Murthy et al., 2003). Interestingly, *sec5* larvae also show growth arrest of neuromuscular junctions and impaired motor neuron arborizations on muscles, suggesting a role for the exocyst complex in regulating the normal development of terminal innervation sites (Murthy et al., 2003). Neurite branching is characterized by the splaying apart and fragmentation of microtubules and by filopodial activity (Gallo and Letourneau, 2004), events that we observe upon Ral activation. Interestingly, local destabilization of microtubules along axons can promote plasma membrane addition, and the exocyst complex has been shown to inhibit tubulin polymerization in vitro (Wang et al., 2004). In normal rat kidney cells, overexpression of the exocyst subunit exo70 results in disruption of the microtubule network and increased plasma membrane addition in the form of long and thin plasma membrane protrusions (Wang et al., 2004). Thus, recruitment of the exocyst complex by active Ral could promote branching through a dual mechanism involving the coordinated regulation of microtubule dynamics and membrane delivery.

Our data indicate that the association between Ral and PLD plays a crucial role in promoting branching, particularly for RalB. Although Ral has no effect on the activity of PLD in vitro, activation of PLD by v-Src, for example, is Ral dependent (Jiang et al., 1995; Luo et al., 1998). Moreover, interaction of Ral with PLD synergistically enhances Arf6-dependent PLD activation downstream of Ras (Xu et al., 2003), and Arf6 has been implicated in the regulation of both axonal and dendritic branching (Hernandez-Deviez et al., 2004) and in the efficient recycling of β1 integrin (Brown et al., 2001). In addition, GTP-bound Arf6 can promote membrane recycling toward specialized plasma membrane regions by directly interacting with the exocyst subunit Sec10 (Prigent et al., 2003). Arf6 activity has also been consistently associated with the formation of actin-based plasma membrane protrusions (Prigent et al., 2003). Although the existence of a signaling pathway downstream of integrins involving Ral and Arf6 remains to be demonstrated, these intriguing links further point to Ral as an attractive candidate molecule likely to coordinate cytoskeletal reorganization and polarized endocytic recycling in response to extracellular matrix stimuli.

PLD generates phosphatidic acid, a multifunctional lipid that can be further metabolized to other important signaling lipids, such as DAG, which is a PKC activator, and lysophosphatidic acid. Several in vitro studies have suggested that PLD plays a role in neurite outgrowth. PLD expression and activity increase during neuronal differentiation of PC12 cells and the immortalized mouse hippocampal stem cell line HiB5 (Min et al., 2001; Sung et al., 2001). In addition, inhibiting PLD activity impairs L1-stimulated neurite outgrowth in cerebellar granule neurons (Watanabe et al., 2004). Interestingly, PLD1 increasingly associates with PKC-α and -βII during NGF-induced neuronal differentiation of PC12 cells (Min et al., 2001), suggesting that PLD and PKC activities are correlated to induce differentiation. Active Ral might then serve a dual function by recruiting PLD to the membrane and enhancing its activity, leading to PKC activation and subsequent phosphorylation of substrates such as GAP-43. In agreement with this, in models of experimentally induced sprouting such as kainate-induced outgrowth of hippocampal mossy fibers, both PLD and GAP-43 are strongly reexpressed (Zhang et al., 2004). Sprouting responses are usually triggered after injury by the release of diffusible growth factors and the up-regulation of several extracellular matrix molecules, among them laminins, which facilitate adhesion and outgrowth of the sprouting processes. Ral could therefore play an important role in coupling extracellular matrix signals to the cytoskeleton via GAP-43 and to vesicle trafficking via the exocyst complex, ultimately leading to branching.

We show that Ral regulates branching through phosphorylation of GAP-43. GAP-43 is generally considered an intrinsic determinant for neurite outgrowth and plasticity. It is maximally expressed during nervous system development and reinduced in injured and regenerating neural tissues, and it serves to potentiate growth cone and nerve terminal responses to local growth and guidance signals. Its expression is not an absolute requirement for neurite outgrowth either in vitro or in vivo (Aigner and Caroni, 1995; Strittmatter et al., 1995). However, depletion experiments in cultured neurons indicate that GAP-43 greatly promotes adhesion and persistent growth cone spreading and branching (Aigner and Caroni, 1995). Membrane anchoring of GAP-43 through palmitoylation plays a crucial role for its morphogenic effects, possibly promoting its recruitment to specialized membrane microdomains enriched in sphingolipids. Incorporation of a lipidated motif such as the one present in GAP-43 into lipid rafts may create local changes in membrane tension and the extension of filopodial structures (Gauthier-Campbell et al., 2004). We found that overexpressed active Ral (particularly RalB) colocalizes in patches along neurites with endogenous GAP-43 (unpublished data). These patches might represent functional adhesion sites, as GAP-43 has been shown to associate with areas of membrane that are tightly bound to the substrate and belong to the membrane cytoskeletal fraction (Meiri and Gordon-Weeks, 1990). Extracellular matrix–induced localization of integrins in lipid rafts can help generate and maintain a specific signaling environment (Decker et al., 2004). Activation of Ral by integrin stimulation along neurites might help recruit

important branch-promoting effectors, such as the exocyst complex and PLD, to such signaling microdomains.

We found that Ral activation increases phosphorylation of endogenous GAP-43 in cortical neurons. Interestingly, PKC-mediated phosphorylation of GAP-43 correlates with increased stabilization of the interaction between growth cones and substrate and, conversely, unphosphorylated GAP-43 is always found in retracting or collapsing areas (Dent and Meiri, 1992). In addition, NGF-treated PC12 cells lacking endogenous GAP-43 and expressing nonphosphorylatable GAP-43 display abnormalities in long-term adhesion to laminin substrates, surface expression of integrins, and cell morphology, with marked membrane blebbing and varicosities (Meiri et al., 1996). Phosphorylation of GAP-43 by PKC therefore seems to maintain a functional coupling between the plasma membrane and the underlying cytoskeleton. Indeed, phosphorylated GAP-43 can stabilize long actin filaments in vitro (He et al., 1997) and can enhance the accumulation of phosphatidylinositol-4,5-bisphosphate–rich plasmalemmal patches, which are possible sites of signal-induced actin assembly (Laux et al., 2000). Maintenance of phosphorylated GAP-43 induced by local Ral activation might therefore contribute to the stabilization of signaling pathways promoting actin polymerization and, ultimately, branching.

GAP-43 knockout mice display pathfinding defects and perturbed development of cortical maps (Strittmatter et al., 1995; Maier et al., 1999), whereas mice overexpressing GAP-43 show striking spontaneous and lesion-induced nerve sprouting, with highly potentiated terminal arborization during innervation (Aigner et al., 1995). Interestingly, several extracellular matrix molecules are up-regulated after injury to either the peripheral or the central nervous system, among them both laminins and collagens (Ivins et al., 2000). In this context, and given that exposure to laminin activates Ral, it is tempting to speculate that this GTPase could act as a mediator between integrin signaling and GAP-43 to potentiate lesion-induced sprouting. Integrins are critical determinants of basic morphogenesis for many aspects of embryogenesis, including nervous system development. Indeed, they participate in a variety of processes, such as brain lamination, neuroblast migration, and axon navigation and synaptogenesis (Milner and Campbell, 2002). Our data point to Ral as an important molecular link between integrin-dependent signaling and cytoskeletal reorganization in neurons. Further investigation should help clarify the involvement of Ral in axonal pathfinding and synapse formation, events relying on both integrin signaling and branch/filopodia formation.

Materials and methods

All reagents were obtained from Sigma-Aldrich unless otherwise specified. Antibodies used were mouse anti-RalA, rabbit anti-RalB (BD Biosciences), mouse anti–GAP-43 (Autogen Bioclear), rabbit anti–phospho(Ser41)-GAP-43 (Zymed Laboratories), rat anti–α-tubulin (Harlan), rat anti-HA (Roche), mouse anti-myc (clone 9E10), rabbit anti-myc (Research Diagnostics, Inc.), mouse anti–βIII tubulin (Sigma-Aldrich), and rabbit anti-p38 (Santa Cruz Biotechnology, Inc.). Rabbit anti–cGAP-43 (Widmer and Caroni, 1993) was a gift from P. Caroni (Friedrich Miescher Institute, Basel, Switzerland). The PKC inhibitor GF109203X was obtained from Calbiochem. All cell culture media and supplements were obtained from Invitrogen. Alexa fluorescent secondary antibodies and fluorescent phalloidin were purchased from Invitrogen.

Plasmids

All Ral mutant constructs were made by PCR or restriction digestions using standard procedures. RalA28N and -72L were cloned into pRK5-myc for expression in mammalian cells, RalB28N and -23V were amplified by PCR using pBabepuroRalB28N and -23V as templates (a gift from K. Kelly, National Cancer Institute, Bethesda, MD) and the following primers: 5′-tcggatccATGGCTGCCAACAAGAGTAAG-3′ and 5′-agtctagaTCATAGTAAGCAACATCTTTC-3′. PCR fragments were then cloned into the BamHI and XbaI sites of pRK5myc. RalA72L and -B23V mutants were constructed from pRK5-myc-RalA72L and pRK5-myc-RalB23V using the Quickchange mutagenesis kit (Stratagene) and the following PCR primers: 5′-GGAGGACCTGGGATCCTTGGCCTTACACAAAG-3′ and 5′-CTTTGTGTAAGGCCAAGGATCCCAGGTCCTCC-3′ for pRK5-myc-RalA72LΔN11, 5′-GGAGGACCTGGGATCCTTGGCCCTCCACAAGG-3′ and 5′-CCTTGTGGAGGGCCAAGGATCCCAGGTCCTCC-3′ for pRK5-myc-RalB23VΔN11, 5′-GCCTACCAAAGCAGAAAGCTACCGGAAGAAGG-3′ and 5′-CCTTCTTCCGGTAGCTTTCTGCTTTGGTAGGC-3′ for pRK5-myc-RalA72LD49E, 5′-GCCTACCAAAGCAAACAGCTACCGGAAGAAGG-3′ and 5′-CCTTCTTCCGGTAGCTGTTTGCTTTGGTAGGC-3′ for pRK5-myc-RalA72LD49N, 5′-CCTACCAAAGCTGAAAGTTATAGAAAGAAAGTGG-3′ and 5′-CCACTTTCTTTCTATAACTTTCAGCTTTGGTAGG-3′ for pRK5-myc-RalB23VD49E, and 5′-CCTACCAAAGCTAACAGTTATAGAAAGAAAGTGG-3′ and 5′-CCACTTTCTTTCTATAACTGTTAGCTTTGGTAGG-3′ for pRK5-myc-RalB23VD49N. pMT2-HA-Rlf-CAAX and pMT2-HA-Rlf-ΔCAT-CAAX were a gift from J. Bos (University of Utrecht, Utrecht, Netherlands). pcDNA3–cGAP-43 (wild type), pcDNA3–cGAP-43(S42A), and pcDNA3–cGAP-43(S42D) were provided by P. Caroni. pGEX-2TK-RalBP1-RBD was a gift from L. Feig (Tufts University, Boston, MA). pEGFP-F was obtained from CLONTECH Laboratories, Inc.

Cell culture

COS-7 cells were maintained in DME supplemented with 10% FCS, 100 IU/ml penicillin, and 100 μg/ml streptomycin and incubated at 37°C and 10% CO_2. Cells were transfected using GeneJuice (Novagen) according to the manufacturer's instructions. Sympathetic neurons were isolated from SCG of newborn Sprague-Dawley rats. Cells were plated on 35-mm plastic dishes or 12-mm glass coverslips coated with 150 μg/ml polyornithine and 10 μg/ml laminin at a density of 30,000 cells/coverslip for immunofluorescence and at least 200,000 cells/dish for Ral-GTP pull-down experiments. For experiments on different substrates, plastic dishes were coated with polyornithine only or with polyornithine and 100 $\mu g/cm^2$ collagen. Neurons were maintained at 37°C at 5% CO_2 in L-15 medium plus 5% FCS, 2 mM glutamine, 24 mM $NaHCO_3$, 100 U/ml penicillin, 50 U/ml streptomycin, 38 mM glucose, 5 ng/ml 7S NGF (Alomone Labs), and 10 μM cytosine arabinoside to restrict glial cell growth. Brain cortices were dissected from E18 rat embryos and dissociated by incubation with 0.05% trypsin-EDTA (Invitrogen) for 20 min at 37°C followed by washing and trituration in DME plus 10% FCS. Dissociated neurons were nucleofected with a primary neuron nucleofection kit (Amaxa) according to the supplier's instructions. Cells were then plated on 35-mm plastic dishes or glass coverslips coated with polyornithine. Medium was replaced 2–3 h after nucleofection with neurobasal medium containing B27 supplement, 2 mM glutamine, and 35 mM glucose. In some experiments, 8 μM of the PKC inhibitor GF109203X or DMSO as control were added at the time of medium replacement and incubated overnight until preparation of neuronal lysates.

Microinjection and immunofluorescence

2 h after plating, constructs were injected at 0.1 μg/μl into the nucleus of cells over a period of 15 min and allowed to express overnight. In laminin-addition experiments, neurons were microinjected 2 h after plating only on polyornithine and left to express for at least 4 h before adding laminin to the medium (final concentration 50 μg/ml) to stimulate neurite outgrowth and branching. 24 h after microinjection, neurons were fixed in 3.7% paraformaldehyde and 20% sucrose in PBS for 15 min at room temperature. After rinsing twice in PBS, cells were incubated for 20 min with 50 mM NH_4Cl in PBS, washed, blocked, and permeabilized with 0.1% Triton X-100, 2% BSA, 0.25% porcine skin gelatin, 0.2% glycine, and 15% FCS in PBS for 15 min at room temperature. Cells were then incubated for at least 1 h at room temperature with primary antibodies diluted in PBS containing 1% BSA and 0.25% porcine skin gelatin (antibody buffer). After rinsing, cells were incubated for 25 min with fluorescent secondary antibodies diluted 1:200 in antibody buffer. Coverslips were mounted on slides with fluorescence mounting medium (DakoCytomation). Fluorescent and phase-contrast images were captured with a charged-coupled device camera (C4742-95; Hamamatsu) connected either to an inverted microscope (DM IRB; Leica) equipped with a 10× 0.25 NA N-Plan objective or

to a microscope (Axioskop; Carl Zeiss MicroImaging, Inc.) equipped with 10× 0.30 NA, 40× 1.30 NA, and 63× 1.25 NA Plan Neofluar objectives. Confocal pictures were acquired using a confocal system (MRC 1024; Bio-Rad Laboratories) with an ILT Krypton Argon laser connected to a microscope (Optiphot 2; Nikon) equipped with 40× 1.0 NA and 60× 1.40 NA Plan Apo objectives. Images were acquired using either Openlab 3.1.7 (Improvision) or Laser Sharp 2000 (Bio-Rad Laboratories) softwares and processed using Photoshop 6.0 (Adobe) or Metamorph 6.0 (Molecular Devices). In some cases, the brightness and contrast of whole images were adjusted to increase the visibility of neurites. Cell profiles were traced manually using Metamorph 6.0. Quantitative analysis of branching in SCG neurons was performed by counting all clearly visible neurite branches >10 μm long. The number of branches per neurite was then calculated by dividing the total number of branches by the number of main neurites (at least twice the length of the cell body diameter) extending from the cell body. For each construct or condition tested, between 30 and 180 neurons from three or more independent experiments were considered. Statistical analysis was performed using a Kruskal-Wallis nonparametric analysis of variance test and Dunn's post-hoc tests with InStat software 2.0 (GraphPad Software).

For RNAi experiments in cortical neurons, quantitative analysis of branching was performed by counting the number of branches positive for tubulin staining extending from the major neurite of those neurons with a clear polarized morphology. Statistical analysis was performed on at least 60 cells per condition from a total of four experiments.

RNAi

Freshly dissociated cortical neurons were nucleofected with 9 μg of siRNA duplexes targeting either the RalA sequence AGACTACGCTGCAATTAGA or the RalB sequence CGCTCCAGTTCATGTATGA (Dharmacon). As a control, a scramble siRNA duplex targeted against GFP (QIAGEN) was used. Cells were fixed 50 h after nucleofection and stained for RalA, RalB (1:50), and tubulin (1:200).

Measurement of GTP-bound state of endogenous Ral and GAP-43 phosphorylation levels

Neuronal lysates were analyzed for the presence of the active form of Ral (Ral-GTP) by affinity purification using a GST fusion with the Ral binding domain of RalBP1 (GST–RalBP1-RBD) immobilized on glutathione-agarose beads as described previously (Tian et al., 2002). To measure the phosphorylation levels of GAP-43, cells were washed twice on ice with cold PBS and scraped in lysis buffer (20 mM Tris-HCl, pH 7.6, 100 mM NaCl, 1% Triton X-100, 12 mM β-glycerophosphate, 5 mM EGTA, 0.5% deoxycholate, 1 mM DTT, 10 mM NaF, 1 mM Na_3VO_4, and 1 mM PMSF). After adding Laemmli buffer, lysates were boiled, sonicated, and analyzed by SDS-PAGE and Western blotting. Immunoblots were visualized with anti-RalA or anti–phospho-GAP-43 antibodies and ECL (GE Healthcare). Quantification by optical density was performed using Quantity One software (Bio-Rad Laboratories).

Online supplemental material

Fig. S1 shows a Western blot analysis of neurons nucleofected with Ral siRNA. Fig. S2 shows that active Ral causes filopodial sprouting from neuronal cell bodies. Fig. S3 shows that adhesion to laminin stimulates GAP-43 phosphorylation. Fig. S4 shows that Ral influences PKC-mediated GAP-43 phosphorylation. Online supplemental material is available at http://www.jcb.org/cgi/content/full/jcb.200507061/DC1.

We thank J. Bos, P. Caroni, L. Feig, and K. Kelly for plasmids and reagents; A. Jaffe, J. Cau, L. Collin, and A. Gärtner for helpful advice on protocols and image analysis; and G. Passmore and D. Brown for SCG culture protocols. We also thank the members of the Hall and Goda Laboratories, Y. Fujita, E. Lalli, G. Lesa, M. Raff, A. Riccio, and G. Schiavo for valuable discussions and comments on the manuscript.

This work was supported by a Wellcome Trust project grant to A. Hall and G. Lalli (069534/z/02/z).

Submitted: 13 July 2005
Accepted: 31 October 2005

References

Acebes, A., and A. Ferrus. 2000. Cellular and molecular features of axon collaterals and dendrites. *Trends Neurosci.* 23:557–565.

Aigner, L., and P. Caroni. 1995. Absence of persistent spreading, branching, and adhesion in GAP-43–depleted growth cones. *J. Cell Biol.* 128:647–660.

Aigner, L., S. Arber, J.P. Kapfhammer, T. Laux, C. Schneider, F. Botteri, H.R. Brenner, and P. Caroni. 1995. Overexpression of the neural growth-associated protein GAP-43 induces nerve sprouting in the adult nervous system of transgenic mice. *Cell.* 83:269–278.

Bhattacharya, M., A.V. Babwah, C. Godin, P.H. Anborgh, L.B. Dale, M.O. Poulter, and S.S. Ferguson. 2004. Ral and phospholipase D2-dependent pathway for constitutive metabotropic glutamate receptor endocytosis. *J. Neurosci.* 24:8752–8761.

Bomze, H.M., K.R. Bulsara, B.J. Iskandar, P. Caroni, and J.H. Skene. 2001. Spinal axon regeneration evoked by replacing two growth cone proteins in adult neurons. *Nat. Neurosci.* 4:38–43.

Brown, F.D., A.L. Rozelle, H.L. Yin, T. Balla, and J.G. Donaldson. 2001. Phosphatidylinositol 4,5-bisphosphate and Arf6-regulated membrane traffic. *J. Cell Biol.* 154:1007–1017.

Chien, Y., and M.A. White. 2003. RAL GTPases are linchpin modulators of human tumour-cell proliferation and survival. *EMBO Rep.* 4:800–806.

Decker, L., W. Baron, and C. Ffrench-Constant. 2004. Lipid rafts: microenvironments for integrin-growth factor interactions in neural development. *Biochem. Soc. Trans.* 32:426–430.

Dent, E.W., and K.F. Meiri. 1992. GAP-43 phosphorylation is dynamically regulated in individual growth cones. *J. Neurobiol.* 23:1037–1053.

Dent, E.W., F. Tang, and K. Kalil. 2003. Axon guidance by growth cones and branches: common cytoskeletal and signaling mechanisms. *Neuroscientist.* 9:343–353.

Dent, E.W., A.M. Barnes, F. Tang, and K. Kalil. 2004. Netrin-1 and semaphorin 3A promote or inhibit cortical axon branching, respectively, by reorganization of the cytoskeleton. *J. Neurosci.* 24:3002–3012.

Feig, L.A. 2003. Ral-GTPases: approaching their 15 minutes of fame. *Trends Cell Biol.* 13:419–425.

Gallo, G., and P.C. Letourneau. 2004. Regulation of growth cone actin filaments by guidance cues. *J. Neurobiol.* 58:92–102.

Gauthier-Campbell, C., D.S. Bredt, T.H. Murphy, and D. El-Husseini Ael. 2004. Regulation of dendritic branching and filopodia formation in hippocampal neurons by specific acylated protein motifs. *Mol. Biol. Cell.* 15:2205–2217.

Goi, T., G. Rusanescu, T. Urano, and L.A. Feig. 1999. Ral-specific guanine nucleotide exchange factor activity opposes other Ras effectors in PC12 cells by inhibiting neurite outgrowth. *Mol. Cell. Biol.* 19:1731–1741.

He, Q., E.W. Dent, and K.F. Meiri. 1997. Modulation of actin filament behavior by GAP-43 (neuromodulin) is dependent on the phosphorylation status of serine 41, the protein kinase C site. *J. Neurosci.* 17:3515–3524.

Hernandez-Deviez, D.J., M.G. Roth, J.E. Casanova, and J.M. Wilson. 2004. ARNO and ARF6 regulate axonal elongation and branching through downstream activation of phosphatidylinositol 4-phosphate 5-kinase alpha. *Mol. Biol. Cell.* 15:111–120.

Ivins, J.K., P.D. Yurchenco, and A.D. Lander. 2000. Regulation of neurite outgrowth by integrin activation. *J. Neurosci.* 20:6551–6560.

Jiang, H., J.Q. Luo, T. Urano, P. Frankel, Z. Lu, D.A. Foster, and L.A. Feig. 1995. Involvement of Ral GTPase in v-Src-induced phospholipase D activation. *Nature.* 378:409–412.

Jullien-Flores, V., Y. Mahe, G. Mirey, C. Leprince, B. Meunier-Bisceuil, A. Sorkin, and J.H. Camonis. 2000. RLIP76, an effector of the GTPase Ral, interacts with the AP2 complex: involvement of the Ral pathway in receptor endocytosis. *J. Cell Sci.* 113: 2837–2844.

Laux, T., K. Fukami, M. Thelen, T. Golub, D. Frey, and P. Caroni. 2000. GAP43, MARCKS, and CAP23 modulate $PI(4,5)P_2$ at plasmalemmal rafts, and regulate cell cortex actin dynamics through a common mechanism. *J. Cell Biol.* 149:1455–1472.

Luo, L. 2002. Actin cytoskeleton regulation in neuronal morphogenesis and structural plasticity. *Annu. Rev. Cell Dev. Biol.* 18:601–635.

Luo, J.Q., X. Liu, P. Frankel, T. Rotunda, M. Ramos, J. Flom, H. Jiang, L.A. Feig, A.J. Morris, R.A. Kahn, and D.A. Foster. 1998. Functional association between Arf and RalA in active phospholipase D complex. *Proc. Natl. Acad. Sci. USA.* 95:3632–3637.

Maier, D.L., S. Mani, S.L. Donovan, D. Soppet, L. Tessarollo, J.S. McCasland, and K.F. Meiri. 1999. Disrupted cortical map and absence of cortical barrels in growth-associated protein (GAP)-43 knockout mice. *Proc. Natl. Acad. Sci. USA.* 96:9397–9402.

Meiri, K.F., and P.R. Gordon-Weeks. 1990. GAP-43 in growth cones is associated with areas of membrane that are tightly bound to substrate and is a component of a membrane skeleton subcellular fraction. *J. Neurosci.* 10:256–266.

Meiri, K.F., J.P. Hammang, E.W. Dent, and E.E. Baetge. 1996. Mutagenesis of ser41 to ala inhibits the association of GAP-43 with the membrane skeleton of GAP-43-deficient PC12B cells: effects on cell adhesion and the composition of neurite cytoskeleton and membrane. *J. Neurobiol.*

29:213–232.

Milner, R., and I.L. Campbell. 2002. The integrin family of cell adhesion molecules has multiple functions within the CNS. *J. Neurosci. Res.* 69:286–291.

Min, D.S., B.H. Ahn, D.J. Rhie, S.H. Yoon, S.J. Hahn, M.S. Kim, and Y.H. Jo. 2001. Expression and regulation of phospholipase D during neuronal differentiation of PC12 cells. *Neuropharmacology.* 41:384–391.

Morris, A.J., M.A. Frohman, and J. Engebrecht. 1997. Measurement of phospholipase D activity. *Anal. Biochem.* 252:1–9.

Moskalenko, S., D.O. Henry, C. Rosse, G. Mirey, J.H. Camonis, and M.A. White. 2002. The exocyst is a Ral effector complex. *Nat. Cell Biol.* 4:66–72.

Moskalenko, S., C. Tong, C. Rosse, G. Mirey, E. Formstecher, L. Daviet, J. Camonis, and M.A. White. 2003. Ral GTPases regulate exocyst assembly through dual subunit interactions. *J. Biol. Chem.* 278:51743–51748.

Murthy, M., D. Garza, R.H. Scheller, and T.L. Schwarz. 2003. Mutations in the exocyst component Sec5 disrupt neuronal membrane traffic, but neurotransmitter release persists. *Neuron.* 37:433–447.

Ngsee, J.K., L.A. Elferink, and R.H. Scheller. 1991. A family of ras-like GTP-binding proteins expressed in electromotor neurons. *J. Biol. Chem.* 266:2675–2680.

Oestreicher, A.B., P.N. De Graan, W.H. Gispen, J. Verhaagen, and L.H. Schrama. 1997. B-50, the growth associated protein-43: modulation of cell morphology and communication in the nervous system. *Prog. Neurobiol.* 53:627–686.

Polzin, A., M. Shipitsin, T. Goi, L.A. Feig, and T.J. Turner. 2002. Ral-GTPase influences the regulation of the readily releasable pool of synaptic vesicles. *Mol. Cell. Biol.* 22:1714–1722.

Prigent, M., T. Dubois, G. Raposo, V. Derrien, D. Tenza, C. Rosse, J. Camonis, and P. Chavrier. 2003. ARF6 controls post-endocytic recycling through its downstream exocyst complex effector. *J. Cell Biol.* 163:1111–1121.

Quilliam, L.A., J.F. Rebhun, and A.F. Castro. 2002. A growing family of guanine nucleotide exchange factors is responsible for activation of Ras-family GTPases. *Prog. Nucleic Acid Res. Mol. Biol.* 71:391–444.

Shen, Y., L. Xu, and D.A. Foster. 2001. Role for phospholipase D in receptor-mediated endocytosis. *Mol. Cell. Biol.* 21:595–602.

Shipitsin, M., and L.A. Feig. 2004. RalA but not RalB enhances polarized delivery of membrane proteins to the basolateral surface of epithelial cells. *Mol. Cell. Biol.* 24:5746–5756.

Strittmatter, S.M., C. Fankhauser, P.L. Huang, H. Mashimo, and M.C. Fishman. 1995. Neuronal pathfinding is abnormal in mice lacking the neuronal growth cone protein GAP-43. *Cell.* 80:445–452.

Sugihara, K., S. Asano, K. Tanaka, A. Iwamatsu, K. Okawa, and Y. Ohta. 2002. The exocyst complex binds the small GTPase RalA to mediate filopodia formation. *Nat. Cell Biol.* 4:73–78.

Sung, J.Y., S.Y. Lee, D.S. Min, T.Y. Eom, Y.S. Ahn, M.U. Choi, Y.K. Kwon, and K.C. Chung. 2001. Differential activation of phospholipases by mitogenic EGF and neurogenic PDGF in immortalized hippocampal stem cell lines. *J. Neurochem.* 78:1044–1053.

Tian, X., G. Rusanescu, W. Hou, B. Schaffhausen, and L.A. Feig. 2002. PDK1 mediates growth factor-induced Ral-GEF activation by a kinase-independent mechanism. *EMBO J.* 21:1327–1338.

Vega, I.E., and S.C. Hsu. 2001. The exocyst complex associates with microtubules to mediate vesicle targeting and neurite outgrowth. *J. Neurosci.* 21:3839–3848.

Wang, S., Y. Liu, C.L. Adamson, G. Valdez, W. Guo, and S.C. Hsu. 2004. The mammalian exocyst, a complex required for exocytosis, inhibits tubulin polymerization. *J. Biol. Chem.* 279:35958–35966.

Watanabe, H., M. Yamazaki, H. Miyazaki, C. Arikawa, K. Itoh, T. Sasaki, T. Maehama, M.A. Frohman, and Y. Kanaho. 2004. Phospholipase D2 functions as a downstream signaling molecule of MAP kinase pathway in L1-stimulated neurite outgrowth of cerebellar granule neurons. *J. Neurochem.* 89:142–151.

Widmer, F., and P. Caroni. 1993. Phosphorylation-site mutagenesis of the growth-associated protein GAP-43 modulates its effects on cell spreading and morphology. *J. Cell Biol.* 120:503–512.

Wolthuis, R.M., N.D. de Ruiter, R.H. Cool, and J.L. Bos. 1997. Stimulation of gene induction and cell growth by the Ras effector Rlf. *EMBO J.* 16:6748–6761.

Xu, L., P. Frankel, D. Jackson, T. Rotunda, R.L. Boshans, C. D'Souza-Schorey, and D.A. Foster. 2003. Elevated phospholipase D activity in H-Ras- but not K-Ras-transformed cells by the synergistic action of RalA and ARF6. *Mol. Cell. Biol.* 23:645–654.

Zhang, Y., P. Huang, G. Du, Y. Kanaho, M.A. Frohman, and S.E. Tsirka. 2004. Increased expression of two phospholipase D isoforms during experimentally induced hippocampal mossy fiber outgrowth. *Glia.* 46:74–83.